Comparison of MIL-STD-1773 Fiber Optic Data Bus Terminals: Single Event Proton Test Irradiation, In-flight Space Performance, and Prediction Techniques

Kenneth A. LaBel[1], Paul W. Marshall[2], Cheryl J. Marshall[3], Janet Barth[1], Henning Leidecker[1], Robert Reed[1], and Christina M. Seidleck[4]

1. NASA/GSFC
2. NRL/SFA
3. NRL
4. Hughes/STX

Abstract

We present a comparison of proton single event ground test results for two generations of MIL-STD-1773 fiber optic data bus interface modules. Single event upset rate prediction techniques for fiber optic data systems are also demonstrated and compared with in-flight space performance.

I. INTRODUCTION AND BACKGROUND

The Hubble Space Telescope (HST) Solid State Recorder (SSR) was recently installed as part of the HST servicing mission (Feb. 14 1997). The SSR utilizes a MIL-STD-1773 fiber optic data bus (hereafter simply called a 1773 bus) to provide command and control message passing internal to the SSR box. For example, the 1773 would be used to send the command and control to transfer a block of science data from an instrument to on-board storage for later shipment to the ground. The 1773 bus [1] has a master-slave structure utilizing an ack-nack protocol. In addition, the 1773 is a redundant system in that there are two data paths for message transfers (i.e., an A side and a B side). A further fault tolerant characteristic is that if a message transfer fails for any reason, the message may be retried from one to three times depending on the specific system implementation. Figure 1 is a block diagram of a 1773 system including protocol devices, transceivers (modules that provide the optical-to-electrical (receiver) and electrical-to-optical (transmitter) interfaces), optical fibers, fiber optic (FO) connectors, and star couplers (devices that distribute the light transmitted to all the optical receivers on that side of the 1773 bus).

The SSR 1773 utilizes second-generation SCI Small Explorer Data System II (SEDSII) modules to provide the optical-to-electrical (receiver) and electrical-to-optical (transmitter) interfaces on each of the SSR cards. The SEDSII module is a repackaging of the original SEDSI modules that also includes a revised radiation hardened (RH) ASIC (LSI Logic's LRH20K process versus the previous LRH10K process). However, in the repackaging process, three other items have changed. The first is a reduced capacitance between the optical receiver Si PIN photodiode and its associated electrical circuitry. The second is an increase in optical receiver sensitivity (~ 3dB). The third is the inclusion of a 24 MHz oscillator inside the hybrid SEDSII module as opposed to being a circuit that is external to the hybrid.

Figure 2 is a generic block diagram of a 1773 transceiver including the LED, photodiode, ASIC device, and oscillator.

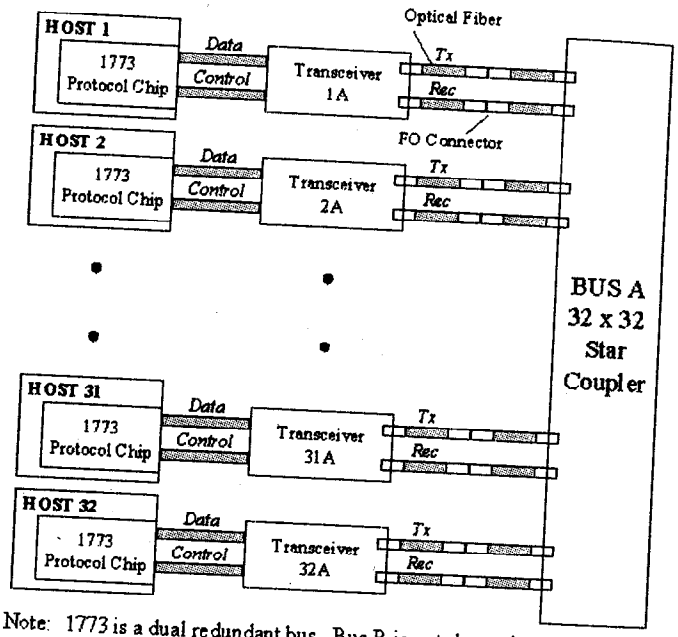

Note: 1773 is a dual redundant bus. Bus B is not shown in this diagram.

Figure 1: Illustrates a representative MIL-STD-1773 system.

Previous testing on the original SEDSI transceiver modules and its associated receiver photodiode [2-6] had shown that essentially every energetic particle that transverses the Si PIN photodiode could create a transient (SET) on the electrical output side of the diode. However, not all of these transients cause an effect external to the receiver. That is, the associated electrical receiver circuitry filters out those transients of insufficient pulsewidth or amplitude to trigger an external observable event. In summary, extensive single event proton ground irradiation testing of the photodiode and the SEDSI modules indicated several things:

- a large portion (>90%) of the diode transients are not observed at the output of the electrical receiver circuitry,
- that light needed to be coupled with the SET in order to cause an event on the 1773 bus; i.e., data transmission must be active for an SET to be noticed by the electrical circuitry of the receiver. Thus, the error rate becomes a function also of the data rate and duty cycle,

0-7803-4071-X/98/$10.00 © 1998 IEEE.

- single message errors are independent of the particle flux rate, while multiple consecutive message errors are dependent on the particle flux rate,
- the amount of optical power incident on the receiver photodiode effects the number of transients observed (more thoroughly summarized in [7,8]),
- an angular incidence effect as well as a proton energy dependence was observed, thus implying direct ionization from protons as the main cause of SETs in the system, and
- error rates for the 1773 system are dominated by the receiver photodiode. Contributions from the transmitter portion of the circuit were several orders of magnitude less than from the receiver.

With these previous results in mind, proton irradiation were undertaken on the receiver portion of the SEDSII modules. Ground irradiation measurements in this paper are discussed in terms of error cross-section as given by equation (1).

$$N \text{ errors} = F \text{ particles/cm}^2 \times \sigma \text{ in cm}^2, \quad (1)$$

where σ is the error cross-section. Several error cross-sections for a given optical link budget or system attenuation were experimentally determined:

- σ_s, which is the error cross-section for a single message error occurring, and
- σ_n, which is the error cross-section for n consecutive messages failing.

For the condition where n=2, σ_n represents the error cross-section for a message retry failing. This will be seen to be of import for in-flight predictions and analyses.

The primary objectives of this investigation were:

- to determine if the SEDSII modules had similar proton SET characteristics as the original SEDSI modules,
- to analyze the in-flight space performance data of the SEDSI and II modules, and
- to perform an analysis of the prediction technique developed for SEDSI performance [4] as it applies to the SEDSII performance. During this phase of the investigation, an alternate approach to predict in-flight space performance was proposed and evaluated.

II. PROTON GROUND IRRADIATION OF THE SEDSII MODULES

A. Test Setup

An engineering test unit (ETU) card from the HST SSR was utilized as a test fixture for the devices under test (DUTs). In addition, a PC-based tester was interfaced via the optical fiber bus and a 6x6 star coupler in order to simulate HST's system and to detect the occurrence of errors during transmissions. Table I shows the nominal optical link budgets, which indicate the amount of optical power (or power lost) between a transmitter and a receiver, for the SEDSII in-flight and test systems as well as the SEDSI system reported on previously [2].

Table 1. Comparison of optical link budgets for 1773 systems under investigation

	SEDSII Test System	SEDSII HST In Flight System	SEDSI as in SAMPEX System
Optical Link Budget (nominal) in dB of loss	13.5	9.5	17.5

The differences in the optical link budgets are due primarily to the size (i.e., number of taps) of the passive star couplers and the number of connectors utilized in the system links. This optical link budget affects the amount of optical power that is incident on the photodiode, thus affecting receiver error performance in a manner that increases error rates as loss over the optical link increases. In this manner, the SEDSII Test System with its higher link loss will be a worst-case approximation of the HST In-flight System.

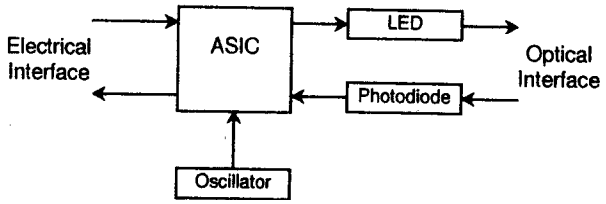

Figure 2: Block diagram of a representative FO transceiver interface.

Multiple other factors were varied during testing including the data (or message) rate and the angle of incidence between the proton beam and the planar surface of the photodiode. For reference, the photodiode is a thin spherical planar device. What is usually considered normal beam incidence enters the photodiode perpendicular to the planar surface. As pointed out earlier, all of the above factors will affect the radiation-induced error rate performance.

B. Test facility

The University of California at Davis (UCD) Crocker Nuclear Laboratory (CNL) cyclotron was utilized for testing. This facility is capable of producing energetic protons up to maximum energy of 63 MeV (incident on the DUT). This prime energy was utilized in the test.

C. SEDSII Test Results for single message errors

1) Data rate and angular incidence effects

Figure 3 plots the single message error cross-section for the tested data rates at each beam incidence angle. The y-axis is a logarithmic scale of single message error cross-section, while the x-axis is a linear scale of the bus data rate in bits per second (bps). As expected based on [2-4], the device single message error sensitivity showed a relative linearity to data rate, i.e., error cross-sections increase linearly with data rate. Additionally, angular incidence effects track the chord length

distributions through the photodiode in a manner similar to that noted in [4].

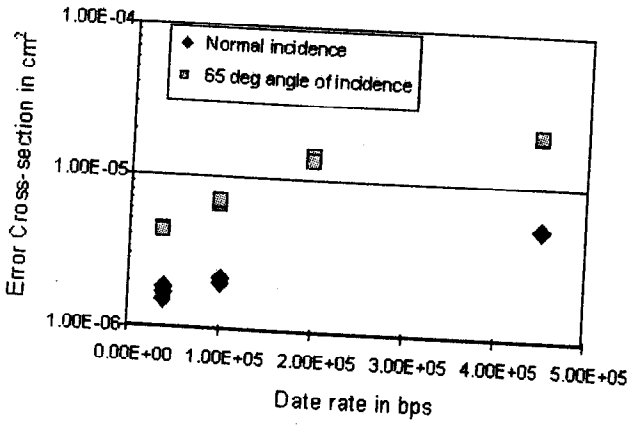

Figure 3 SEDSII error cross-section as a function of data rate: two different angles of incidence.

2) *Optical attenuation effects*

Figures 4 and 5 are representative plots of the message error cross-section dependence on system optical link budgets. On the linear-scaled x-axis in these plots, the numbers on the x-axis represent the induced attenuation beyond the nominal system with 0 dB representing the nominal test system. That is, 4 dB on the x-axis implies an additional 4 dB of system attenuation (from the nominal 13.5 dB to 17.5 dB). The y-axis is a logarithmic scale of single message error cross-section. Figure 4 illustrates this optical power dependence for a 21 kbps data rate at normal incidence. Figure 5 is a similar graph for multiple data rates at a 65 degree beam incidence angle. The message error cross-section is fairly insensitive to additional induced loss until greater than ~ 3 or 4 dB of induced attenuation is added. After this optical power level is reached, single message error cross-section increases as further optical attenuation is induced. Since the optical link attenuation budget for the in-flight HST SEDSII system is less than that of the test system, the nominal test system without additional induced attenuation represents the worst case condition for estimating the HST 1773 in-flight performance.

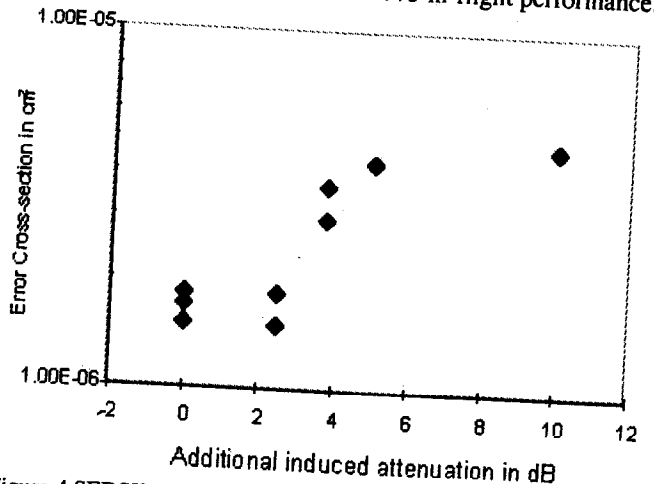

Figure 4 SEDSII message error cross-section for various induced attenuation levels: normal incidence, 21 kbps data rate

3) *Particle flux rate effects*

No particle flux rate dependence was observed for single message error cross-sections; i.e., the measured cross-section is independent of proton flux. This is as expected from [2-4].

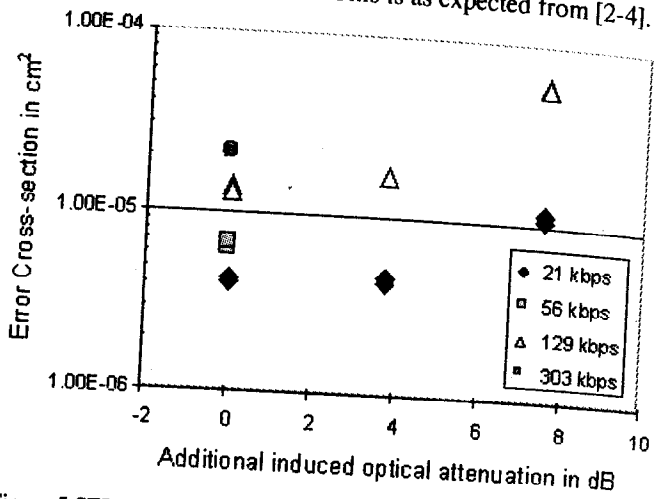

Figure 5 SEDSII message error cross-section for various induced attenuation levels: 65 degree incidence angle

D. *SEDSII Test Results for consecutive message errors (retry failures)*

1) *Data rate and particle flux effects*

Previous results [4] showed that for a given optical link budget,

$$\sigma_n = (\sigma_s^n \times \psi^{n-1}) / MR^{n-1} \quad (2)$$

where MR is the message rate in messages per second and ψ is the particle flux in particles per cm^2 per second. Thus, a dependence on data rate (message rate) and flux rate are inherent in the system for consecutive message errors (n=2). Note that σ_s is the special case where n=1. Figure 6 illustrates these points from the SEDSI data set. The SEDSII data set similarly followed the above relationship.

2) *Optical attenuation and angular incidence effects*

As with the single message error cross-sections, the optical link budget and angular incidence affected the results. Figure 7 illustrates a sample of the data collected. As with the single message error cross-sections, as optical attenuation was increased, so too did the error cross-sections. The angular incidence effect also performed in a manner similar to the single message error tests. Please note that in Figure 7, the error cross-sections at nominal (0 dB) optical attenuation are limiting cross-sections in that no errors were observed during the test runs.

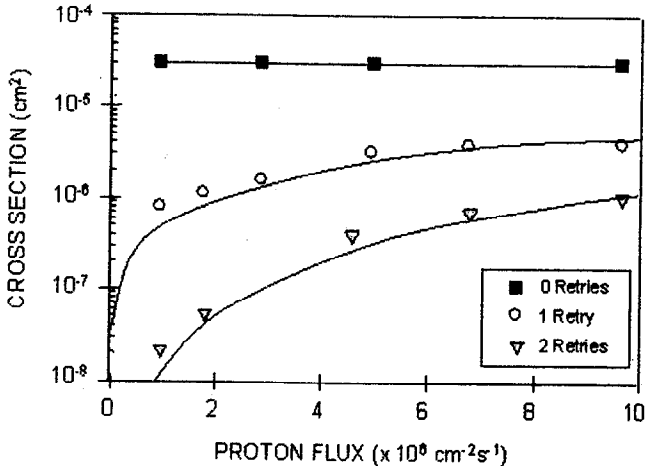

Figure 6: 1773 SEDSI Error cross-section vs. flux for 0, 1, 2 retries: 161 kbps data rate normal attenuation.

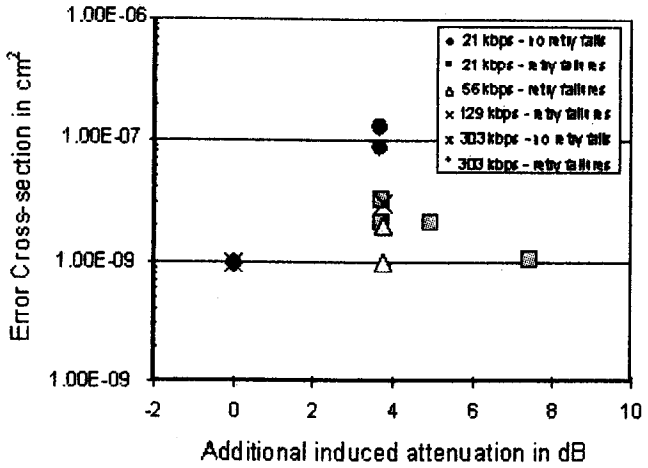

Figure 7: SEDSII Retry failure (n=2) error cross-sections for varying optical link budget scenarios: normal incidence angle and varying data rates

III. COMPARISON OF SEDSI AND SEDSII TEST RESULTS

In order to compare the two sets of test results, normalization of the test factors such as data rate, angular incidence, particle flux rates, and optical attenuation must be considered. For example as shown in Table 1, the SEDSI test system had a 4 dB greater system optical attenuation than the SEDS II test system. This is mostly due to the use of a 16x16 passive star coupler in the SEDSI test set as opposed to the 6x6 in the HST test system. When these factors are normalized the test results between the SEDSI and SEDSII devices are very similar. Figure 8 illustrates the SEDSI and SEDSII single message error cross-sections versus tested data rate for a normalized optical link budget (the SEDSI budget) and a proton beam incidence angle of 45 degrees. This is a linear-linear plot with the y-axis showing single message error cross-section and the x-axis the data rate. It is apparent from this figure that data points from the SEDSI and SEDSII follow a linear relationship when the gathered proton radiation data is normalized for a "common" test configuration. This commonality between the SEDSI and SEDSII modules was also shown to be true when considering message retry scenarios. Thus even with several design changes, the SEDSII terminals do not behave significantly different than the SEDSI devices from the proton-induced SEU perspective.

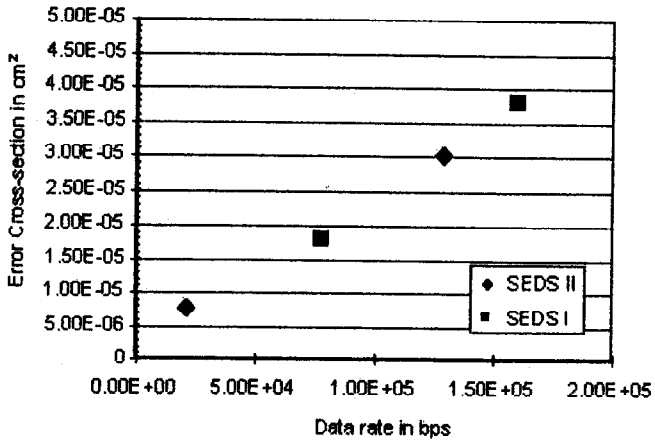

Figure 8 Comparison of SEDSI and SEDSII message error cross-sections after normalization: SEDSI system optical attenuation, 45 degree incidence angle, various data rates

IV. IN-FLIGHT PERFORMANCE

This section presents some of the in-flight performance data that exists for the SEDSI and SEDSII modules. The SEDSI devices were used in the Solar Anomalous Magnetospheric Particle Explorer (SAMPEX) satellite (a Polar orbiting spacecraft), while, as pointed out earlier, the SEDSII hybrids are utilized for HST (a low-inclination satellite). The data shown in the associated graphs plot the number of retried messages (bus retries) which are an indicator of a single message error.

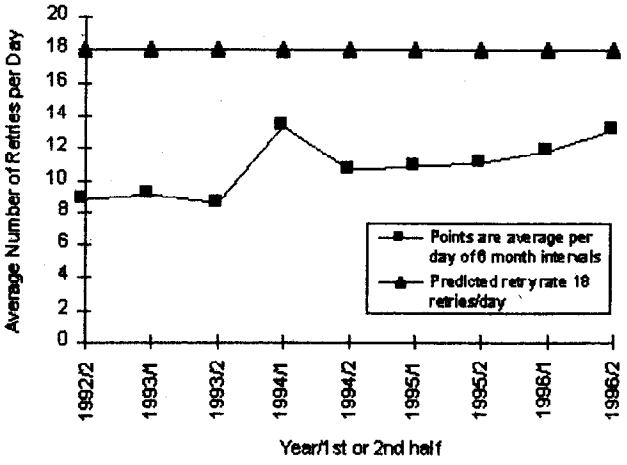

Figure 9 In-flight number of bus retries per day for SAMPEX

A. *SAMPEX Performance*

Figure 9 presents the average number of bus retries per day observed for six month periods of time from launch in July 1992 until December 1996 for the SEDSI-based system

used on SAMPEX. Averages are between 9-14 retries per day and are within a factor of 2 of the worst-case analysis utilized in [4] for mission predictions. One might note the increase over time in retry rates; this correlates well with the expected increase in proton fluences as the mission has transitioned from a Solar Maximum to a Solar Minimum period as well as with observed solar flare events.

When retries are enabled in the system, single messages may be retransmitted and successfully passed, thus, only retry failures may affect the mission performance. Since mission inception, only one failed retry has occurred for SAMPEX. This data is in excellent agreement with the pre-flight prediction of one per seven years.

B. *HST Performance*

Figure 10 presents the number of bus retries per day observed for the first two months of SEDSII-based system performance on the HST SSR. Daily bus retry variations are intrinsically due to the orbital precession, thus causing a variance in the daily proton fluences.

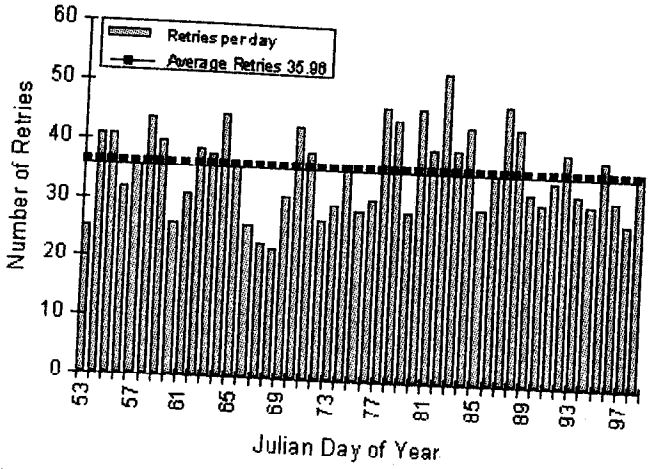

Figure 10 HST SEDSII bus retries per day for March-April 1997

Since the installation of the SSR on-board the HST, retry failures have occurred at the approximate rate of one every 2 days. This retry failure rate is not in good agreement with the models and ground irradiation test data nor with the SAMPEX in-flight performance. Predictions, as shown in the next section, are for orders of magnitude lower failure rates. Thus, these retry failures are not radiation-induced anomalies, but more than likely a secondary system (hardware or software) implementation issue. It should be noted that even with an occasional failed retry, the HST SSR is fully operational.

V. PREDICTION TECHNIQUES

Predictions were performed for the new HST SSR SEDSII modules using the method outlined in [4]. A second novel method utilizing physical photodiode dimensions was also explored

A. *HST SSR SEDSII Predictions Using Existing Method*

From [2], knowing that the data rate dependence is given in the measured single message error cross-sections and that single message error upsets are independent of flux, then for HST, the probability of a single message error is

$$P_s = (\sigma_s \times \psi)/MR \quad (3)$$

where σ_s = error cross-section for a single message error = 4E-6 cm^2 (based on ground radiation testing)

ψ = particle flux = 1.076E7 protons/cm^2/day for protons of E > 25 MeV [9]

MR = message rate = 630 messages/sec x 8.64E4 secs/day = 5.5E7 messages/day

Thus, $P_s = (\sigma_s \times \psi)/MR = 7.83$ E-7 (4)

But we know from standard SEU rate equations that the number of single message errors is

$E_s = \sigma_s \times \psi$ = 4E-6 cm^2/message x 1.076E7 p/cm^2/day= 43 single message errors a day. (5)

The actual in-flight single message error rate is: ~ 36 errors/day, thus we have a good correlation between the test data and the in-flight single message error performance.

Now turning towards retry error rates, from [4] we know that

$$P_N = P_s^N = (\sigma_s^N \times \psi^N)/ MR^N, \quad (6)$$

then solving for σ_N,

(5) σ_N = error cross-section for N consecutive messages in error

$$= (\sigma_s^N \times \psi^{N-1})/ MR^{N-1}$$

For N=2 (2 consecutive messages failing or alternately the single retry failure cross-section) and knowing that there is a flux rate dependence for retry errors, we may perform a worst case analysis using the peak proton fluxes for this mission,

for a ψ of 2E3 protons/cm^2/sec for E >25 MeV [9],

$$\sigma_2 = 5.1\text{E-}11\ cm^2.$$

Again using the standard SEU rate calculation methods, but this time for the worst-case retry failure rate,

$E_N = \sigma_N \times \psi$ = 1.02E-7 retry fails/sec (7)

Since we know that the total fluence of protons is 1.076E7 protons/cm^2/day for protons of E > 25 MeV and the peak flux is 2E3 protons/cm^2/sec, we may extend [4] by assuming (again worst-case) that all the protons seen daily are entered at the peak flux rate. Thus, we'd have

# of secs per day seeing protons = fluence/flux=

5380 secs. (8)

If we multiply the retry failure rate per second by the # of seconds/day having protons, we get the fail rate per day

$$FR_{day} = (6) \times (7) = 5.49E\text{-}4 \text{ fails/day or one fail every 5 years.} \quad (9)$$

While this retry failure rate does not agree with the observed retry failure rate for the HST SSR, this prediction method proved to be accurate in predictions for SAMPEX as well as other spacecraft whose data is not presented here.

B. *HST SSR SEDSII Predictions Using a Novel Method*

An alternative method of in-flight predictions was explored using physical diode dimensions as well as the in-flight message error performance to determine single retry error rates. We are given the following known data:

SA = surface area of the diode = 6.4 E-3 cm^2

Bus Utilization of the 1Mbps 1773 bus for HST (including 50% duty cycle effect of Manchester encoded data streams) = BU = 0.0189 or 1.89%

MD = message duration = 30E-6 seconds for the HST SSR system.

We may define a hit rate (HR) such that,

$$HR = SA \times \psi \quad (10)$$

This is stating the number of particles incident on the surface of the PIN photodiode in the optical receiver.

We may then define an error rate of single message errors,

$$E_s = BU \times SA \times \psi \times F, \text{ where F = the \% of particle hits that are not filtered by the electronic receive circuitry that follows the PIN photodiode (i.e. propagated errors).} \quad (11)$$

We are currently observing ~ 37 single message errors a day for the HST SSR. If we let E_s = 37, and solving (10) for F, we get F = 2.84 E-2 or less than 3% of the diode hits are being detected as having an effect on the receive circuitry output. For additional accuracy, we would need longer period of data to determine F as well as a proton fluence monitor. A similar method may be performed, however, utilizing the ground irradiation test data.

In a manner analogous to the worst-case analysis using the existing prediction technique, for a worst-case peak flux condition, we may define the probability of a single message error by the receiver as

$$P_s = MD \times HR \times F = 30E\text{-}6sec \times (6.4E\text{-}3cm^2 \times 2E3 \; p/cm^2/sec) \times 2.84E\text{-}2 = 1.09E\text{-}5 \quad (12)$$

Since single message errors are mutually exclusive random events, we know that the probability of two consecutive messages failing (single retry failure) is,

$$P_2 = P_s^2 = 1.19E\text{-}10 \quad (13)$$

Again, we may solve for the retry failure rate per second,

$$FR_{sec} = P_s^2 \times MR = 1.19E\text{-}10 \times 630 \text{ messages/sec} = 7.50E\text{-}8 \text{ fails/sec.} \quad (14)$$

As in the worst-case analysis for the existing prediction method, assuming all 1.076E7 protons/cm^2/day are delivered in 5380 secs, the actual retry fail rate per day is

$$FR_{day} = FR \times \text{\# of proton-secs/day} = 7.50E\text{-}8 \times 5380 = 4.03E\text{-}4 \text{ fails/day or one every 6.8 years.} \quad (15)$$

Thus, this method provides a reasonable correlation (< 50% variance) for HST versus the existing SEU rate method in [4]. A similar analysis for SAMPEX provides equally accurate results.

VI. CONCLUSIONS

We have provided a comparison of test data for two generations of 1773 bus modules as well as a correspondence of in-flight performance. In addition, we have shown the accuracy of predicting message errors and single retry failures using standard and novel techniques.

However, there is still the anomaly of excessive retry failures for the HST SSR. Simply because all the retry errors occur during HST's passes through the proton belts, it is not sufficient reason to blame the problem on the radiation-induced anomalies in the SEDSII modules. It is strongly pointed out that since single message errors only occur in the this region of HST's orbit, message retries are only performed there. Thus, the retry error is symptomatic of radiation only. If the retries occurred in other portions of the orbit, it is possible that the same type of retry error would occur regardless of the radiation environment. A latent system design flaw or other anomalous condition or radiation sensitive device would then be suspected.

VII. ACKNOWLEDGMENTS

The authors would like to thank Ali Feizi and Keith Kienzle of Jackson and Tull for their efforts in performing the ground experiments. In addition, we would like to acknowledge the support of Steven Horowitz and the HST project as well as NASA HQ and DSWA.

VIII. REFERENCES

[1] "Fiber Optics Mechanization of an Aircraft Internal Time Division Command/Response Multiplex Data Bus," MIL-STD-1773, May 1988.

[2] K. A. LaBel, E.G. Stassinopoulos, and G.J. Brucker, "Transient SEUs in a Fiber Optic System for Space Applications", IEEE Trans. on Nucl. Sci., Vol. NS-38, pp. 1546-1550, Dec 1991.

[3] K.A. LaBel, E.G. Stassinopoulos, P. Marshall, E. Petersen, C.J. Dale, C. Crabtree, and C. Stauffer, "Proton irradiation SEU test results for the SEDS MIL-STD-1773 fiber optic data bus: integrated optoelectronics", Proc. SPIE 1953, pp. 27-36, 1993.

[4] K.A. LaBel, P. Marshall, C. Dale, C.M. Crabtree, E.G. Stassinopoulos, J.T. Miller, and M.M. Gates, "SEDS MIL-STD-1773 fiber optic data bus: Proton irradiation test results and spaceflight SEU data", IEEE Trans. on Nuc. Sci., Vol. NS-40 pp 1638-1644, Dec. 1993.

[5] C.M. Crabtree, K.A. LaBel, E.G. Stassinopoulos, J.T. Miller, "Preliminary SEU Analysis of the SAMPEX MIL-STD-1773 Spaceflight Data", Proc. SPIE, Vol. 1953, pp. 37-44, 1993.

[6] C.M. Seidleck, K.A. LaBel, A.K. Moran, M.M. Gates, J.L. Barth, and E.G. Stassinopoulos, "Single Event Effect Flight Data Analysis of SAMPEX , XTE, and Other NASA Missions: Solid State Recorder and Fiber Optic Bus Performance", presented at the Tenth SEE Symposium, Apr 1996.

[7] P.W. Marshall, C.J. Dale, E.J. Friebele, and K.A. LaBel, "Survivable fiber-based data links for satellite radiation environments", SPIE Critical Review CR-14, Fiber Optics Reliability and Testing, pp. 189-231, 1994.

[8] P.W. Marshall, C.J. Dale, K.A. LaBel, "Space radiation effects in high performance fiber optic data links for satellite management", IEEE Trans. on Nuclear Science, vol 43, no. 2, pp. 645-653, April 1996.

[9] Private communication, GSFC's Radiation Physics Office, Mar 1997.